Carrier-Concentration Dependence of the Pseudogap Ground State of Superconducting $Bi_2Sr_{2-x}La_xCuO_{6+\delta}$ Revealed by ^{63,65}Cu-Nuclear Magnetic Resonance in Very High Magnetic Fields

Shinji Kawasaki,[1] Chengtian Lin,[2] Philip L. Kuhns,[3] Arneil P. Reyes,[3] and Guo-qing Zheng[1,4]

[1]*Department of Physics, Okayama University, Okayama 700-8530, Japan*
[2]*Max-Planck-Institut fur Festkorperforschung, Heisenbergstrasse 1, D-70569 Stuttgart, Germany*
[3]*National High Magnetic Field Laboratory, Tallahassee, Florida 32310, USA*
[4]*Institute of Physics and Beijing National Laboratory for Condensed Matter Physics, Chinese Academy of Sciences, Beijing 100190, China*

We report the results of the Knight shift by ^{63,65}Cu-NMR measurements on single-layered copper-oxide $Bi_2Sr_{2-x}La_xCuO_{6+\delta}$ conducted under very high magnetic fields up to 44 T. The magnetic field suppresses superconductivity completely, and the pseudogap ground state is revealed. The ^{63}Cu-NMR Knight shift shows that there remains a finite density of states at the Fermi level in the zero-temperature limit, which indicates that the pseudogap ground state is a metallic state with a finite volume of Fermi surface. The residual density of states in the pseudogap ground state decreases with decreasing doping (increasing x) but remains quite large even at the vicinity of the magnetically ordered phase of $x \geq 0.8$, which suggests that the density of states plunges to zero upon approaching the Mott insulating phase.

The mechanism of the high transition temperature (T_c) superconductivity in copper oxides (cuprates) [1] still remains unclear, largely because the relationship between the normal-state properties and superconductivity is unclear. In conventional metals, superconductivity develops out of a Fermi liquid state. This is also true in the electron-doped n-type cuprates [2]. However, in the normal state of p-type cuprates, there is an intriguing phenomenon called a pseudogap state, in which the density of states (DOS) is depleted upon decreasing temperature (T) below a characteristic temperature T^* [3]. NMR and other measurements have suggested that the pseudogap and superconductivity are coexisting states of matter [4–6], but the detailed properties and the origin of the pseudogap are still under debate [7–10]. Angle-resolved photoemission spectroscopy measurements have suggested that the pseudogap is either associated with disconnected Fermi arcs [5,6], or small Fermi pockets [11,12], or associated with coexisting Fermi arcs and small Fermi pockets [13]. In contrast, there was also a proposal that the Fermi surface shrinks to a nodal point when cooled to $T = 0$ [14]. More importantly, it is still unknown how the pseudogap ground state would evolve as the Mott insulating state is approached.

Experimentally, this is difficult due to the high upper critical field ($H_{c2} \sim 100$ T). In addition, there have been few systems which allow us to explore in a wide doping region. $Bi_2Sr_{2-x}La_xCuO_{6+\delta}$ is one of the ideal systems to study the subject. It has a single CuO_2 layer, highly two-dimensional structure [15], and much lower $T_c^{max} \sim 32$ K compared to other cuprates. Here, La introduces one electron to $Bi_2Sr_2CuO_{6+\delta}$ [16]; hence, "$1 - x$" corresponds to the hole-doping rate.

In this Letter, we report the results of the spin susceptibility via the ^{63,65}Cu-NMR Knight shift measurements in $Bi_2Sr_{2-x}La_xCuO_{6+\delta}$ carried out under very high magnetic fields up to 44 T. When the quantity $1/T_1T$ has a strong T dependence [4], where T_1 is the spin-lattice relaxation time, it is difficult to extract quantitatively the DOS from this quantity. In contrast, the Knight shift is directly proportional to the DOS, which allows us to evaluate the doping dependence of the residual DOS in the pseudogap ground state. We find, for the first time, that an antiferromagnetic order occurs in the strongly underdoped region of this family of compounds. Most importantly, we find that the pseudogap ground state is a metallic state with a finite DOS which decreases with decreasing doping but remains quite large even at the vicinity of the magnetically ordered phase. Our result suggests that the DOS plunges to zero upon approaching the Mott insulating phase.

Single crystalline $Bi_2Sr_{2-x}La_xCuO_{6+\delta}$ samples ($0.0 \leq x \leq 0.9$) are grown by the traveling solvent floating zone method as reported elsewhere [17,18]. Black and shiny single crystal platelets sized up to $\sim 10 \times 3 \times 0.4$ mm^3 cleaved from the as-grown ingot were used. For all measurements, the magnetic field is applied along the c axis. High magnetic fields are generated by the Bitter magnet (21.7–30 T) and the Hybrid magnet (44 T), respectively, in the National High Magnetic Field Laboratory, Tallahassee, Florida. The T dependence of Cu-NMR/nuclear quadrupole resonance intensity $I(0)$ is precisely estimated through a fitting to $I(t) = I(0)\exp(-2t/T_2)$, where T_2 is the nuclear spin-spin relaxation time.

Figure 1 shows the T dependence of the Knight shift [$K_c(T)$] for the $x = 0.40$ sample measured at $H = 7$, 30,
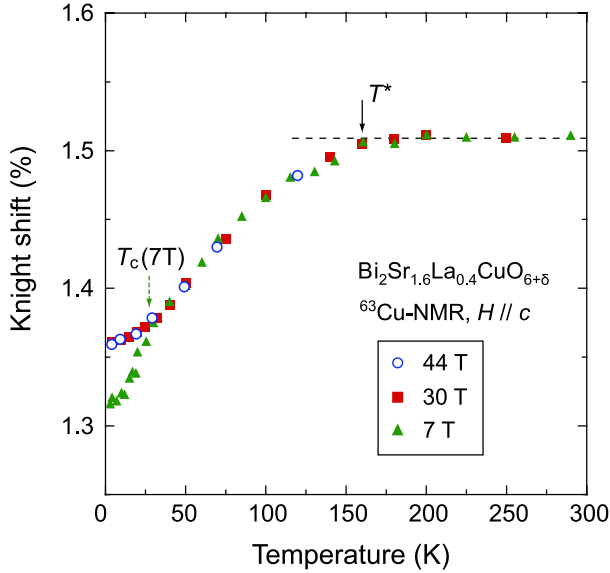
FIG. 1 (color online). T dependence of the ^{63}Cu Knight shift ($H \parallel c$) for $x = 0.40$ measured under different magnetic fields. The solid and dotted arrows indicate the pseudogap temperature T^* and superconducting T_c ($H = 7$ T), respectively. The dotted line is a guide to the eye.

and 44 T, respectively. Here, the obtained $K_c(T)$ is written as $K_c(T) = K_s(T) + K_{orb}$, where K_s and K_{orb} are the shifts due to the spin and the orbital susceptibility, respectively. Generally, K_{orb} is T- and H-independent. Most importantly, K_s and K_{orb} are expressed as $K_s(T) = A_{hf}^s \chi_s(T)$ and $K_{orb} = A_{hf}^{orb} \chi_{orb}$, respectively, where A_{hf} is the hyperfine coupling constant.

At high-T region, K_c does not depend on T, which is consistent with the observation of a full Fermi surface above T^* [19]. As indicated in the figure, K_c starts to decrease below $T^* \sim 160$ K. Notably, $1/T_1T$ for $x = 0.40$ also starts to decrease below T^* [4]. These results indicate a certain loss of the DOS at the Fermi surface taking place below T^*, i.e., the opening of a pseudogap. This T dependence of K_c is consistent with other high-T_c cuprates [20]. As seen in the figure, T^* is almost field-independent. At $H = 7$ T, K_c decreases abruptly below $T_c(H) \sim 30$ K due to the reduction of the spin susceptibility as a result of a spin-singlet Cooper pairing. However, at $H = 30$ and 44 T, no signature of a superconducting transition is observed, as in previous T_1 measurement [4]. Also, the value of K_c at the lowest T is H-independent between $H = 30$ and 44 T. This indicates that the superconductivity is suppressed by fields $H \geq 30$ T and that the T dependence of K_c ($H \geq 30$ T) represents the property of the pseudogap ground state. Importantly, K_c is quite large in the $T = 0$ limit. Namely, the pseudogap ground state has a finite residual DOS. Furthermore, no internal magnetic field is found when superconductivity is destroyed.

We study the doping evolution of the residual DOS by performing the same measurements for other samples with

different x. Figure 2 shows the summary of T dependence of $K_c(T)$ for $0.0 \leq x \leq 0.75$ after suppressing superconductivity by the magnetic field. At high T, the constant value of K_c increases systematically with increasing hole doping (decreasing La content). As shown by arrows in the figure, T^* can be clearly identified, below which K_c starts to decrease, for $0.10 \leq x \leq 0.75$.

In order to quantitatively evaluate the residual DOS in the pseudogap ground state, one needs to estimate K_{orb}, which we find to be 1.21% as elaborated below. In the superconducting state, $K_c = K_s + K_{orb} + K_{dia}$. $K_{dia} = -H_{dia}/H$ is the contribution due to the diamagnetism in the vortex state, which is estimated by using the relation $H_{dia} = (\phi_0/4\pi\lambda_{ab}\lambda_c)\ln(\beta e^{-1/2}d/\sqrt{\xi_{ab}\xi_c})$ [21], where ϕ_0 is the flux quantum, λ is the penetration depth, d is the vortex distance, and $\beta = 0.381$ [21]. We have used $\lambda_{ab} = 4000$ Å, $\lambda_c = 10\lambda_{ab}$ [22], $\xi_{ab} = 35$ Å, and the relation $\lambda_c/\lambda_{ab} = \xi_{ab}/\xi_c$. The value of ξ_{ab} is extracted from $H_{c2}(H \parallel c) \sim 26$ T obtained in the present work.

Figure 3 shows the field dependence of K_c for $x = 0.40$ at $T \sim 2$ K. K_s at $T \ll T_c$ in the superconducting state contains the contribution from nodal quasiparticles which is H-dependent and that due to impurity scattering [23]. The former in the absence of impurity is proportional to $\sqrt{H}$, namely, $K_c(H) - K_{dia} = K_{orb} + K_H\sqrt{H/H_{c2}}$ [24], which is shown as a dotted curve in Fig. 3. The latter is not negligible for the present sample, since $1/T_1T$ well below T_c remains finite even at $H = 0$ [4]. To account for both effects in the dirty limit, we employed the theoretical
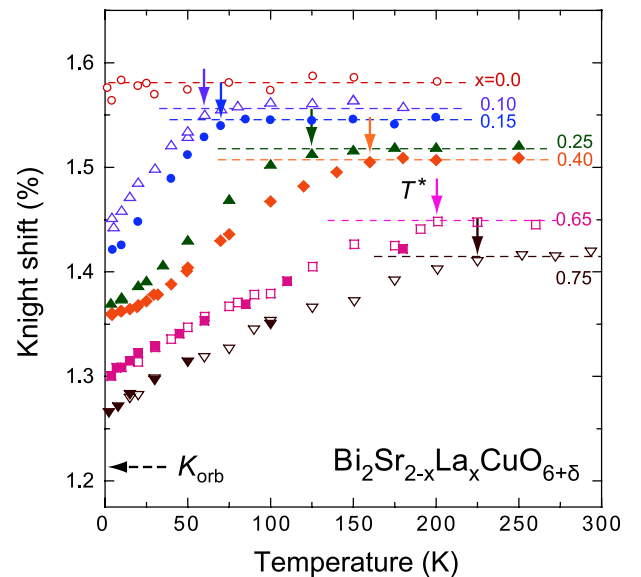

FIG. 2 (color online). T dependence of K_c for $0.0 \leq x \leq 0.75$. The open symbols are results measured at 9 T. The closed symbols are taken at different fields as follows: 30 (for all $x \geq 0.15$), 21.7 (for $x = 0.65$ and 0.75), and 44 T (for $x = 0.40$). The solid arrows indicate the pseudogap temperature T^*. The dotted lines are guides to the eye. The dotted arrow indicates the value of K_{orb} (see text).
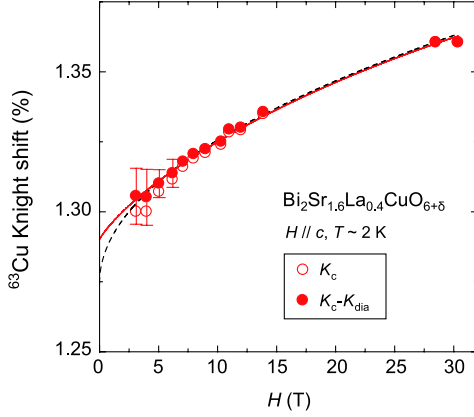
FIG. 3 (color online). Field dependence of K_c and $K_c - K_{dia}$ for $x = 0.40$. The dotted and solid curves are fittings assuming $K_c(H) - K_{dia} \propto \sqrt{H}$ in the absence of impurity scattering and $K_c(H) - K_{dia} \propto \frac{H}{H_{c2}} \ln(\frac{H_0}{H})$ in the presence of impurity scattering, respectively.

model: $K_c(H) \propto \frac{H}{H_{c2}} \ln(\frac{H_0}{H})$ [25], where H_0 is a cutoff energy [25]. This model has succeeded in reproducing the field dependence of K_c for $TlSr_2CaCu_2O_{6.8}$ [26]. As shown by the solid curve in Fig. 3, the relation $K_c - K_{dia} = 1.29\% + 0.0261 [\frac{H}{26.3} \ln(\frac{338}{H})]$ can reproduce experimental results reasonably well. The value of 1.29% is the sum of K_{orb} and the impurity-induced spin shift K_s^{imp}. From the relation $1.29\% = K_{orb} + (\delta n_{imp}/n_0)(1.38\% - K_{orb})$, we obtained the value of $K_{orb} = 1.21\%$. Here, $\delta n_{imp}/n_0 = 0.468$ is the value extracted from T dependence of $1/T_1 T$ at $H = 0$ [4] by using theoretical calculation [26,27], and 1.38% is the value of K_c at $T_c = 32$ K. The obtained value of $K_{orb} = 1.21\%$ is comparable to other high-T_c cuprates [20]. Thus, we can extract the residual DOS $N_{res}(E_F) \propto K_s(T = 0) = K_c(T = 0) - K_{orb}$ from the results in Fig. 2. The results will be discussed later.

Meanwhile, we turn to the strongly underdoped samples, $x = 0.90$ and 0.80, which do not show superconductivity. Figure 4(a) shows the T dependences of ^{63,65}Cu-NMR/ nuclear quadrupole resonance intensity times T. Generally, $I(T)$ increases in proportion to $1/T$. Therefore, the quantity $I(T) \times T$ must be constant. Actually, it is T-independent down to $T_c(H)$ for $x = 0.75$. However, it decreases upon cooling below $T = 60$ and 140 K for $x = 0.80$ and 0.90, respectively. In addition, as seen in Fig. 4(b), we further found a zero-field NMR spectrum at low T induced by the internal magnetic field (H_{int}) at the Cu site. These results evidence the occurrence of anti-ferromagnetic order with $T_N = 60$ K for $x = 0.80$ and $T_N = 140$ K for $x = 0.90$. The spectrum can be modeled with a quadrupole-perturbed Zeeman transition with parameters: $H_{int} = 7.2$ T, $^{63}\nu_Q(^{65}\nu_Q) = 31.7(29.3)$ MHz, and $\theta = 57°$. Here, the nuclear spin Hamiltonian is given as $\mathcal{H}_{AFM} = -\gamma \hbar \vec{I} \cdot \vec{H}_{int} + (h\nu_Q/6)[3I_z^2 - I(I + 1)]$, and θ is the angle between the z axis and H_{int}. These
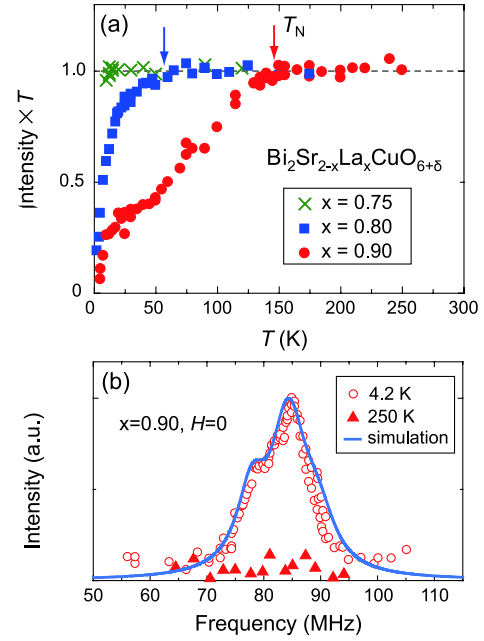

FIG. 4 (color online). (a) T dependences of $I(T) \times T$ for $x = 0.75$, 0.80, and 0.90, respectively. The data are normalized by the value at high temperatures. The dotted line is a guide to the eye. The arrows indicate T_N. (b) Zero-field ^{63,65}Cu-NMR spectrum above and below T_N for $x = 0.90$. The solid curve is a fit to a model described in the text.

parameters are in good agreement with previous results in the insulating phase of $Bi_2Sr_2CuO_6$ [28]. It is noted that the system with $x \gtrsim 0.8$ is in the insulating state as evidenced by resistivity measurements [18].

Now we discuss the main finding. The upper panel of Fig. 5 shows the phase diagram obtained through the present work together with T^* determined by our T_1 measurements [4]. T^* for $x = 0.90$ is determined only by T_1 measurement [29]. The hole concentration in $Bi_2Sr_{2-x}La_xCuO_{6+\delta}$ was evaluated by Ono et $al.$ [18] from the Hall coefficient (upper horizontal scale) and has been used quite widely [30]. From the T dependence of $K_s(T)$, we obtained the doping dependence of T^*. At $x = 0$, a metallic state is established [4]. From $x = 0.10$ to 0.90, notably, $K_s(T)$ and $1/T_1 T$ indicate almost the same T^*. For $x = 0.80$ and 0.90, antiferromagnetic order sets in although T^* still exists at $T^* = 250$ K for $x = 0.90$.

The lower panel of Fig. 5 shows the evolution of residual DOS for the pseudogap ground state. The vertical axis is the relative DOS, N_{res}/N_0, at $T = 0$ as defined by $N_{res}/N_0 = K_s(T = 0)/K_s(T = T^*)$. For $x > 0$, this quantity contains the contribution released by suppressing superconductivity and the contribution by impurity scattering which does not change when the superconductivity is suppressed. The latter contribution is about 0.1% and is almost x-independent. For $x = 0$, the system is in a conventional metallic state, which remains true when the superconductivity is suppressed. For $x \gtrsim 0.1$, a pseudogap
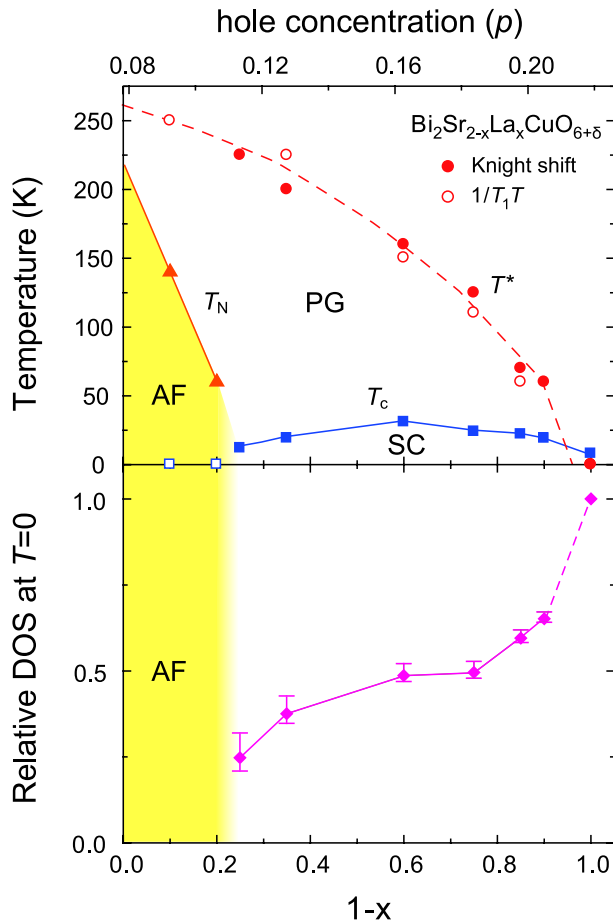
FIG. 5 (color online). The upper panel shows characteristic temperatures vs $1 - x$ ($\propto$ hole concentration). For $x = 0.90$ and 0.80, no superconductivity occurs (open squares). The open circles are taken from Refs. [4,29]. The lower panel shows the hole-concentration dependence of relative DOS at $T = 0$.

opens and causes the partial loss of the DOS. The relative DOS continuously decreases with decreasing hole concentration. It is interesting that the relative DOS remains quite large ($\sim 25\%$) even at $x = 0.75$, which is very close to the Mott state at $x = 0.80$.

The result suggests that the residual DOS for the pseudogap ground state will vanish abruptly as the Mott insulating phase is approached. Recent experiment suggests that a symmetry breaking may occur in the pseudogap state [31]. Our result puts a constraint on the searching for such symmetry breaking. Namely, any symmetry breaking, if it would occur, should not be accompanied by an appearance of an internal magnetic field. Furthermore, the relative DOS we found in this experiment ($\sim 25\%$) is much larger than that inferred from the quantum oscillation ($\sim 3\%$) [11].

In conclusion, NMR measurements under very high magnetic fields up to 44 T reveal the antiferromagnetically ordered state in the strongly underdoped region and the doping evolution of the pseudogap ground state in

$Bi_2Sr_{2-x}La_xCuO_{6+\delta}$. Our result indicates that the pseudogap ground state is a metallic state with a finite DOS which decreases with decreasing doping but remains quite large even at the vicinity of the Mott insulating phase. The present work revealed the complete phase diagram for a single-layered high-T_c cuprate.

[1] J. G. Bednorz and K. A. Müller, Z. Phys. **64**, 189 (1986).
[2] G. -q. Zheng et al., Phys. Rev. Lett. **90**, 197005 (2003).
[3] For a review, see T. Timusk and B. Statt, Rep. Prog. Phys. **62**, 61 (1999).
[4] G. -q. Zheng et al., Phys. Rev. Lett. **94**, 047006 (2005).
[5] K. Tanaka et al., Science **314**, 1910 (2006).
[6] T. Yoshida et al., Phys. Rev. Lett. **103**, 037004 (2009).
[7] K.-Y. Yang, T. M. Rice, and F.-C. Zhang, Phys. Rev. B **73**, 174501 (2006).
[8] H. Kondo and T. Moriya, J. Phys. Soc. Jpn. **78**, 013704 (2009).
[9] S. Sakai, Y. Motome, and M. Imada, Phys. Rev. Lett. **102**, 056404 (2009).
[10] T. Senthil and P. A. Lee, Phys. Rev. B **79**, 245116 (2009).
[11] N. Doiron-Leyraud et al., Nature (London) **447**, 565 (2007).
[12] A. F. Bangura et al., Phys. Rev. Lett. **100**, 047004 (2008).
[13] Jianqiao Meng et al., Nature (London) **462**, 335 (2009).
[14] A. Kanigel et al., Nature Phys. **2**, 447 (2006).
[15] N. L. Wang et al., Phys. Rev. B **47**, 3347 (1993).
[16] J. Akimitsu et al., Jpn. J. Appl. Phys. **26**, L2080 (1987).
[17] B. Liang and C. T. Lin, J. Cryst. Growth **267**, 510 (2004).
[18] S. Ono et al., Phys. Rev. Lett. **85**, 638 (2000).
[19] M. R. Norman et al., Nature (London) **392**, 157 (1998).
[20] K. Asayama et al., Prog. Nucl. Magn. Reson. Spectrosc. **28**, 221 (1996), and references therein.
[21] P. G. de Gennes, Superconductivity of Metals and Alloys (Benjamin, New York, 1966).
[22] P. L. Russo et al., Phys. Rev. B **75**, 054511 (2007).
[23] Y. Sun and K. Maki, Phys. Rev. B **51**, 6059 (1995).
[24] G. E. Volovik, JETP Lett. **58**, 469 (1993).
[25] I. Vekhter, P. J. Hirschfeld, and E. J. Nicol, Phys. Rev. B **64**, 064513 (2001).
[26] G. -q. Zheng et al., Phys. Rev. Lett. **88**, 077003 (2002).
[27] N. Bulut and D. J. Scalapino, Phys. Rev. Lett. **67**, 2898 (1991).
[28] M. Kato, K. Yoshimura, and K. Kosuge, J. Solid State Chem. **133**, 372 (1997).
[29] S. Kawasaki et al. (unpublished).
[30] Y. Wang et al., Science **299**, 86 (2003).
[31] M. Hashimoto et al., Nature Phys. **6**, 414 (2010).